CNS Neuroscience & Therapeutics

ORIGINAL ARTICLE

Different Patterns of Spontaneous Brain Activity between Tremor-Dominant and Postural Instability/Gait Difficulty Subtypes of Parkinson's Disease: A Resting-State fMRI Study

Hui-Min Chen,[1,2] Zhi-Jiang Wang,[3] Jin-Ping Fang,[1,2] Li-Yan Gao,[1,2] Ling-Yan Ma,[1,2] Tao Wu,[4,5] Ya-Nan Hou,[4,5] Jia-Rong Zhang[4,5] & Tao Feng[1,2,4]

1 Center for Neurodegenerative Disease, Department of Neurology, Beijing Tiantan Hospital, Capital Medical University, Beijing, China
2 China National Clinical Research Center for Neurological Diseases, Beijing, China
3 State Key Laboratory of Cognitive Neuroscience and Learning & IDG/McGovern Institute for Brain Research, Beijing Normal University, Beijing, China
4 Parkinson's Disease Center, Beijing Institute for Brain Disorders, Capital Medical University, Beijing, China
5 Department of Neurobiology, Key Laboratory on Neurodegenerative Disorders of Ministry of Education, Beijing Institute of Geriatrics, Xuanwu Hospital, Capital Medical University, Beijing, China

Keywords
Amplitude of low-frequency fluctuations (ALFF); Parkinson's disease; Postural instability/gait difficulty (PIGD); Resting-state fMRI; Tremor.

Correspondence
T. Feng, Center for Neurodegenerative disease, Department of Neurology, Beijing Tiantan Hospital, Capital Medical University, No. 6 Tian Tan Xi Li Street, 100050 Beijing, China. Tel.: +86-139-1112-5339;
Fax: +86-10-6709-8052;
E-mail: happyft@sina.com
Received 1 June 2015; revision 21 August 2015; accepted 24 August 2015

doi: 10.1111/cns.12464

The first two authors contributed equally to this work.

SUMMARY

Aims: Postural instability/gait difficulty (PIGD) and tremor-dominant (TD) subtypes of Parkinson's disease (PD) show different clinical manifestations; however, their underlying neural substrates remain incompletely understood. This study aimed at investigating the subtype-specific patterns of spontaneous brain activity in PD. **Methods:** Thirty-one patients with PD (12 TD/19 PIGD) and 22 healthy gender- and age-matched controls were recruited. Resting-state functional magnetic resonance imaging data were collected, and amplitude of low-frequency fluctuations (ALFF) was measured. Voxelwise one-way analysis of covariance and *post hoc* analyses of ALFF were performed among the three groups, with age and gender as covariates (levodopa daily dosage and gray matter volume as additional covariates for validation analysis). Correlations of clinical variables (e.g., disease duration and PIGD/tremor subscale score) with ALFF values were examined. **Results:** Compared with controls, patients with TD exhibited higher ALFF in the right cerebellar posterior lobe and patients with PIGD exhibited lower ALFF in the bilateral putamen and cerebellar posterior lobe, and higher values primarily in several cortical areas including the inferior and superior temporal gyrus, superior frontal, and parietal gyrus. Compared with patients with PIGD, patients with TD had higher ALFF in the bilateral putamen and the cerebellar posterior lobe, as well as lower ALFF in the bilateral temporal gyrus and the left superior parietal lobule. In all patients, ALFF in the bilateral cerebellar posterior lobe positively correlated with tremor score and ALFF in the bilateral putamen negatively correlated with PIGD score. **Conclusion:** Different patterns of spontaneous neural activity in the cerebellum and putamen may underlie the neural substrate of PD motor subtypes.

Introduction

Parkinson's disease (PD) is a progressive neurodegenerative disorder, the main clinical manifestations of which include bradykinesia, tremor, rigidity, and gait/postural disturbance. Based on clinical phenotypes, PD can be further divided into tremor-dominant (TD), postural instability/gait difficulty (PIGD), and mixed subtypes [1]. The PIGD subtype is characterized by predominantly axial motor involvement, and has a more rapid deterioration of motor function and lower response to levodopa or deep brain stimulation treatments than the TD subtype [1–4]. A previous study using positron emission tomography (PET) showed that the TD subtype of PD is associated with increased metabolism in the cerebellum/dentate nucleus, primary motor cortex, and the caudate/putamen [5]. Another radiotracer study using single photon emission computed tomography (SPECT) demonstrated that patients with PIGD had more severe presynaptic dopamine function in the putamen than both patients with TD and healthy controls [6]. However, the neural substrate underlying these motor subtypes of PD is not particularly well understood.

Recently, resting-state functional magnetic resonance imaging (R-fMRI) has been widely used to examine brain function in both normal and pathological conditions, given the physiological importance of intrinsic or spontaneous brain activity during

low-frequency (0.01−0.1 Hz) fluctuations of the blood oxygen level-dependent signal during rest [7–9]. Zang et al. (2007) proposed an important R-fMRI metric of amplitude of low-frequency fluctuations that can reflect the intensity of spontaneous neural activity at rest [10]. Recently, ALFF abnormality has been detected in brain diseases, including PD [11], Alzheimer's disease [12], and schizophrenia [13]. Studies in PD have found alterations in spontaneous brain activity. For instance, Hou et al. (2014) examined ALFF values in different frequency bands and reported lower ALFF in the putamen in both slow-4 (0.027−0.073 Hz) and slow-5 (0.010−0.027 Hz) frequency bands in patients with PD [11]. Skidmore et al. (2013) reported that patients with PD had decreased ALFF in the supplementary motor cortex, the mesial prefrontal cortex, the right middle frontal gyrus, and the left cerebellar lobule VII/VIII, as well as increased ALFF in the right cerebellar lobule IV/V [14]. These findings suggest that altered spontaneous brain activity may reflect the pathophysiology of PD to a certain degree. However, these studies did not consider disparate presentations of PD subtypes. Using R-fMRI, a recent study by Zhang et al. (2015) compared TD and akinetic/rigid-predominant subtypes of PD and found distinct regional homogeneity patterns of spontaneous brain activity in the striato-thalamo-cortical loop and the cerebello-thalamo-cortical loop between these two subtypes of PD [15]. Their results highlight the distinguishable neural substrate underlying different subtypes of PD. However, more evidence is needed to delineate spontaneous neural activities for the motor subtypes of PD.

Clinically, the PIGD subtype displays poor prognosis [1]. An investigation of the neural substrate in the PIGD subtype is critical to improve the clinical management of the PIGD subtype. Several studies have indicated that relative to patients with TD, patients with PIGD may experience both greater loss of white matter integrity in the bilateral superior longitudinal fasciculus, bilateral anterior corona radiata, and the left genu of the corpus callosum [16] and lower gray matter (GM) volumes in the presupplementary motor and the primary motor areas [17]. Radiotracer studies have shown that a wide range of cortical β-amyloid deposition and forebrain-cortical cholinergic system degeneration may be associated with gait/postural dysfunction in PD [18,19]. However, whether the PIGD subtype has a specific functional pattern of regional brain activity and whether regional brain activities are different between the PIGD and TD subtypes remains to be elucidated.

In this study, we hypothesize that the PD patients with PIGD and TD subtypes would show different patterns of regional brain activity, which may underlie their neural substrates. To address this issue, we used R-fMRI and ALFF to investigate regional differences in spontaneous brain activity in the TD and PIGD subtypes, and to further explore their clinical correlates. Furthermore, we performed a validation analysis by respectively adding levodopa daily dosage and GM volume as additional covariates to assess the potential effects of drug treatment and GM volume.

Materials and Methods

Participants

Fifty-three subjects (12 patients with TD, 19 patients with PIGD, and 22 healthy controls [HC]) participated in this study. Patients with PD were recruited from Xuanwu Hospital, Capital Medical University, Beijing, China. Patients were diagnosed in accordance with the United Kingdom Parkinson's Disease Society Brain Bank (UKPDBB) criteria by two experts on movement disorders [20]. Exclusion criteria were as follows: (i) diagnosis uncertain for PD or suspicious of parkinsonism syndrome (vascular, drug-induced, toxin-induced, postinfectious parkinsonism), multiple system atrophy, corticobasal ganglionic degeneration, or progressive supranuclear palsy; (ii) a history of stroke, moderate-to-severe head trauma, hydrocephalus, brain surgery, or brain tumor; (iii) a contraindication for MRI scan (pacemaker implanted, etc.); (iv) inability to cooperate or communicate; and (v) Mini-Mental State Exam (MMSE) score $\leq$24. Gender- and age-matched healthy controls, recruited from the local community by advertisements, had normal neurological status and movement function, absence of neurological or psychiatric disease, and MMSE >24. All procedures were approved and supervised by the ethics committee of Xuanwu Hospital, Capital Medical University, in accordance with the Declaration of Helsinki. Informed consent was obtained from the participants.

Demographic information, including age, disease duration, Hoehn and Yahr (H-Y) stage, Unified Parkinson's Disease Rating Scale (UPDRS), and levodopa daily dosage, was collected for each patient. The TD and PIGD groups were defined by UPDRS, where the ratio of the mean UPDRS tremor scores [UPDRS item 16, tremor; item 20, rest tremor (face, right upper extremity, left upper extremity, right lower extremity, left lower extremity); item 21, action tremor (right upper extremity, left upper extremity)] to the mean UPDRS PIGD scores (UPDRS item 13, falling; item 14, freezing; item 15, walking; item 29, gait; item 30, postural stability) was calculated. Patients with a ratio >1.5 were classified as TD and ratio <1 as PIGD. Additionally, patients who had a positive mean in the numerator and zero in the denominator were classified as TD; patients with a zero in the numerator and a positive mean in the denominator were classified as PIGD [1].

Data Acquisition

All MRI data were acquired using a SIEMENS Trio 3-Tesla scanner (Siemens, Erlangen, Germany). Foam padding and headphones were used to limit head motion and reduce scanner noise. High-resolution brain structural images were acquired using T1-weighted, sagittal 3D magnetization-prepared rapid gradient echo (MPRAGE) sequences with the following parameters: repetition time (TR)/echo time (TE)/inversion time = 2000 ms/2.19 ms/900 ms; flip angle (FA) = 9°; field of view (FOV) = 224 mm × 256 mm; in-plane resolution = 224 × 256; slice thickness = 1 mm; and 176 sagittal slices. Functional images were collected axially using an echo-planar imaging (EPI) sequence with the following settings: TR/TE = 2000 ms/40 ms; FA = 90°; FOV = 256 mm × 256 mm; resolution = 64 × 64; axial slices = 28; thickness/gap = 4 mm/1 mm; voxel size = 4 × 4 × 5 mm^3; and bandwidth = 2230 Hz/pixel. Prior to the scan, subjects were instructed to keep their eyes closed, relax but not fall asleep, and move as little as possible during scanning. Two lengths of the resting-state fMRI scans were acquired: one was acquired with 239 volumes for all normal controls, 6 patients with TD, and 12

patients with PIGD; and the other was acquired with 300 volumes for the other 6 patients with TD and 7 patients with PIGD. For consistency of time points, we cut off the posterior 61 volumes for the longer time series. In total, we acquired 239 volumes for each of the 22 HC, 12 TD, and 19 PIGD study participants.

Data Preprocessing

All preprocessing was carried out using Statistical Parametric Mapping (SPM8, http://www.fil.ion.ucl.ac.uk/spm) and Data Processing Assistant for R-fMRI (DPARSF, http://www.restfmri.net/forum/DPARSF) toolkits [21]. The first 10 volumes of the functional images were discarded because of signal equilibrium and the participants' adaptation to the scanning circumstance. The remaining 229 volumes were then corrected for intravolume acquisition time delay between slices and for intervolume geometrical displacement due to head motion. Next, the individual T1-weighted images were coregistered to the mean realigned functional images using a linear transformation [22] and were then segmented into GM, white matter, and cerebrospinal fluid tissue maps using a unified segmentation algorithm [23] followed by nonlinear normalization into the Montreal Neurological Institute (MNI) space. With the transformation parameters, the motion-corrected functional volumes were then spatially normalized into the MNI space and resampled to 3-mm isotropic voxels. Next, the nuisance signals of 24 head motion parameters [24], global signal, cerebrospinal fluid, and white matter signals as well as linear trend were regressed out from each voxel's time course. Temporal band-pass filtering (0.01−0.1 Hz) was performed on the residual time series of each voxel to reduce the effect of low-frequency drifts and high-frequency noise [7,25]. Subsequently, resultant functional images were spatially smoothed with a 4 mm full width at half-maximum Gaussian kernel. Finally, no subject was excluded under a head motion criterion of 3 mm and 3°. We also compared their mean framewise displacement estimates of Jenkinson [26] and found no significant difference among the three groups (a one-way ANOVA test, $P = 0.246$).

We used the R-fMRI Data Analysis Toolkit (REST, http://rest.restfmri.net)[27] to calculate ALFF as described in previous studies [10,28]. Briefly, for a given voxel, the time course was first extracted and then converted to a frequency domain using a fast Fourier transformation. The square root of the power spectrum was computed and averaged across the 0.01–0.1 Hz frequency interval. This averaged square root was taken as the ALFF of the given voxel. It was further divided by the global mean value to reduce the global effects of variability across participants. Notably, the ALFF calculation was constrained within a group GM mask that was obtained by selecting a threshold of 0.2 on the mean GM probability map of all 53 subjects.

To explore the possible effect of GM atrophy, we performed a voxel-based morphometry (VBM) for structural images using DARTEL [29]. Spatially normalized GM maps were modulated by the Jacobian determinant of the deformation field and corrected for individual brain sizes. The modulated GM maps were then smoothed using an 8 mm full width at half-maximum Gaussian kernel.

Statistical Analysis

To examine significant differences in ALFF among the three groups, a one-way analysis of covariance (ANCOVA) was performed in a voxelwise manner (within the group GM mask), with age and gender treated as covariant factors. The statistical significance level was set at $P < 0.05$ and cluster size >237 voxels, which corresponded to a corrected $P < 0.05$. To determine between-group ALFF differences, a subsequent *post hoc* analysis with the general linear model (GLM) was further performed (within a mask showing significant group differences in the ANCOVA). The statistical significance level was set at $P < 0.05$ and cluster size >72 voxels, which corresponded to a corrected $P < 0.05$. All multiple comparison corrections were conducted using the AFNI 3dClustSim program (http://afni.nimh.nih.gov/pub/dist/doc/program_help/3dClustSim.html).

To investigate the relationship between ALFF values and clinical scores (i.e., disease duration, UPDRS, H-Y, MMSE, tremor, and PIGD scores), we performed a voxelwise multiple linear regression analysis within the mask showing group differences from the ANCOVA, with age and gender treated as covariates. The statistical significance level was set at $P < 0.05$ and cluster size >49 voxels, corresponding to a corrected $P < 0.05$.

Validation Analysis

To evaluate the effects of drug treatment and GM volume on our results, we reperformed the above-mentioned GLM analysis to test the between-group ALFF differences with levodopa daily dosage and GM volume treated as additional covariates, respectively.

Results

Demographic Profiles

Clinical and demographic data for the 53 study subjects are shown in Table 1. There were no significant differences among the three groups in gender, age, and MMSE score. No significant differences were found between the TD and PIGD subtypes in disease duration, H-Y stage, UPDRS III score, and levodopa daily dosage. However, the patients with TD had significantly higher tremor score than the patients with PIGD, whereas the patients with PIGD exhibited higher PIGD score than patients with TD, in consistency with clinical manifestations of each subtype.

Comparison of ALFF Values among the TD, PIGD, and HC Groups

ANCOVA revealed significant differences in ALFF among the TD, PIGD, and HC groups in several brain regions, involving the cerebellar vermis VIII and the right cerebellar lobule VIII, the bilateral putamen, the bilateral temporal gyrus, the superior frontal gyrus, and the superior parietal lobule ($P < 0.05$, corrected; Figure 1).

Table 1 Demographics of TD, PIGD, and HC groups

	TD (n = 12)	PIGD (n = 19)	HC (n = 22)	*P*
Gender (F:M)	8:4	7:12	10:12	0.263[a]
Age (years)	62.6 ± 8.71 (48–74)	64.8 ± 8.34 (42–76)	65.1 ± 5.00 (58–75)	0.593[a]
Disease duration (years)	6.38 ± 4.01 (2.5–15)	6.68 ± 4.85 (1–22)	–	0.855[b]
H-Y stage	1.87 ± 0.607 (1–3)	2.13 ± 0.984 (0–4)	–	0.363[b]
UPDRS III	19.1 ± 11.5 (6–48)	21.6 ± 11.6 (7–57)	–	0.556[b]
MMSE	28.3 ± 2.67 (25–30)	27.5 ± 2.01 (25–30)	28.6 ± 1.57 (25–30)	0.110[a]
Levodopa daily dosage (mg/day)	302 ± 205 (0–750)	464 ± 284 (125–1000)	–	0.097[b]
Tremor score	6.33 ± 3.37 (3–15)	3.37 ± 2.99 (0–10)	–	0.016[b]
PIGD score	2.17 ± 1.53 (0–6)	5.00 ± 1.97 (2–10)	–	<0.001[b]

TD, tremor-dominant subtype of Parkinson's disease; PIGD, postural instability/gait difficulty subtype of Parkinson's disease; HC, healthy control. MMSE, Mini-Mental State Exam. H-Y stage and MMSE score were analyzed by Mann–Whitney test and gender by chi-square test, and the remainders were tested by ANOVA. [a]Comparisons were made among three groups. [b]Comparisons were made between TD and PIGD groups.

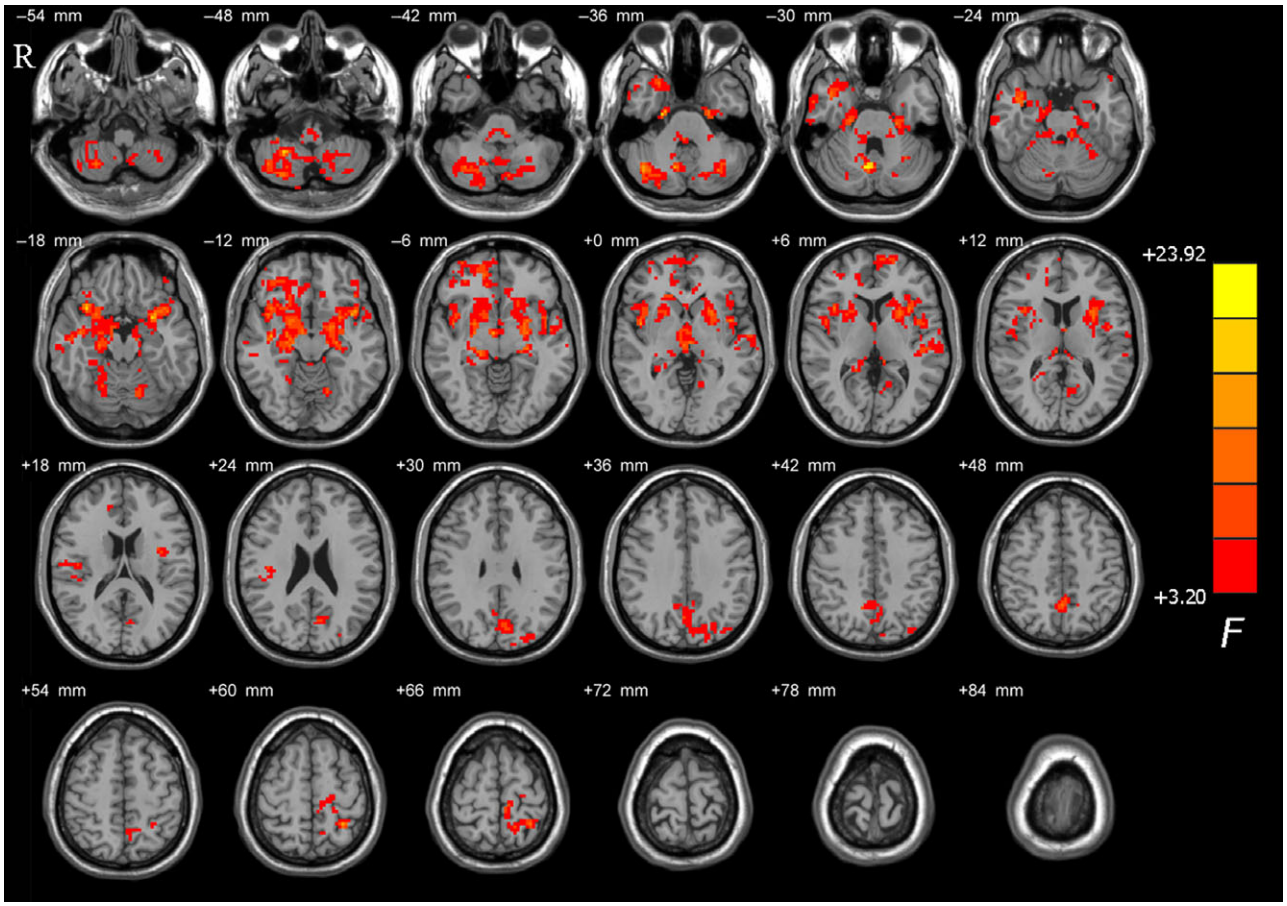

Figure 1 Brain maps for amplitude of low-frequency fluctuations (ALFF) differences among tremor-dominant (TD), postural instability/gait difficulty (PIGD), and healthy control (HC) groups. The statistical significant level was set at $P < 0.05$ and cluster size >237 voxels within the group mean gray mask, which corresponded to a corrected $P < 0.05$. The left side of the image corresponds to the right side of the brain in axial orientation; slice coordinates according to Montreal Neurological Institute (MNI) space are shown in the upper right corner of the slices, indicating Z-axis in axial orientation.

Comparison of ALFF Values between Groups

Compared with the controls, the patients with TD exhibited higher ALFF values in the right cerebellar lobule VIII and the right superior frontal gyrus ($P < 0.05$, corrected; Figure 2A and Table 2). Additionally, we also found that there was a cluster in the cerebellar vermis VIII that survived the height, but not the extent threshold.

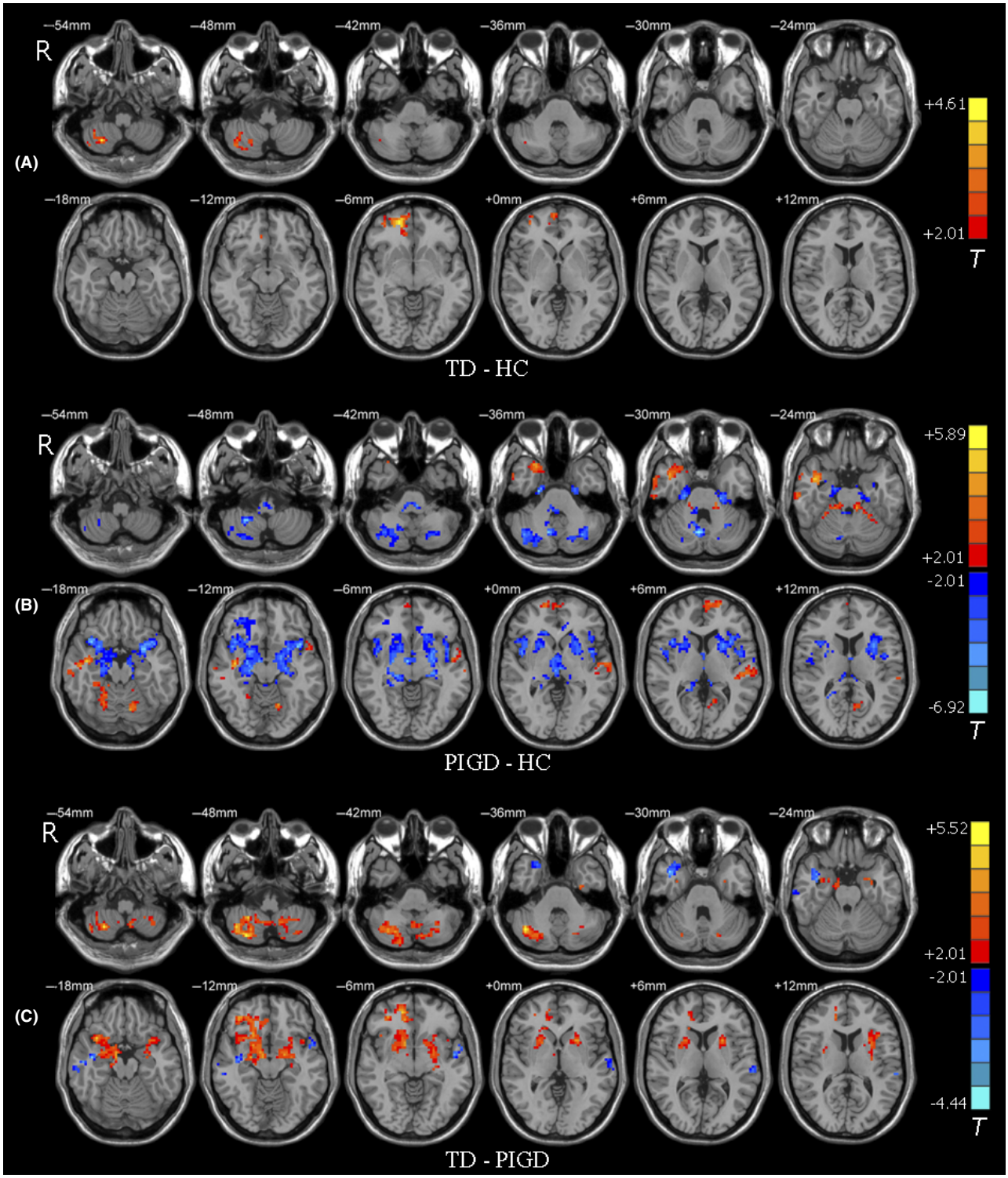

Figure 2 Brain maps for between-group differences in ALFF values. The statistical threshold was set at $P < 0.05$ and cluster size >72 voxels, which corresponds to a corrected $P < 0.05$. (**A**) TD group had higher ALFF values in the right cerebellar lobule VIII and the right prefrontal cortex than HC. Of note, lower ALFF values in the vermis VIII survived the height threshold, but not the extent threshold. (**B**) ALFF differences between PIGD and HC groups. (**C**) ALFF differences between the TD and PIGD groups. The left side of the image corresponds to the right side of the brain in axial orientation; slice coordinates according to MNI space are shown in the upper right corner of the slices, indicating Z-axis in axial orientation. For details of the regions, see Table 2.

Table 2 Between-group differences in regional brain activity

Brain regions	Brodmann area	MNI coordinates (mm)			*T* value	Cluster size
		x	y	z		
TD > HC						
Cerebellum_8_R (aal)		27	−63	−54	4.19	43
Frontal_Sup_R(aal)	BA 11	18	54	−6	4.37	40
PIGD > HC						
Temporal_Sup_L (aal)	BA 22	−54	−24	6	3.88	94
Temporal_inf_R (aal)	BA 20	39	−12	−12	5.14	54
Frontal_Sup_L (aal)	BA 10	−18	63	6	3.92	33
Parietal_Sup_L (aal)	BA 7	−30	−48	63	5.89	12
Cerebellum_4_5_L (aal), Cerebellum_3_L (aal)		−9	−36	−24	4.24	29
PIGD < HC						
Putamen_L (aal)		−27	6	−15	−6.92	154
Putamen_R (aal)		39	15	−15	−6.02	114
Cerebellum_8_R (aal)		6	−66	−30	−6.17	100
Vermis_8 (aal)						
Cerebellum_Crus2_L (aal)		−30	−69	−36	−4.52	71
Brain stem		−6	−33	−42	−5.01	36
TD > PIGD						
Cerebellum_8_R (aal)		42	−66	−36	5.21	129
Putamen_R (aal)		36	42	−9	5.52	109
Putamen_L (aal)		−30	−6	−15	4.22	98
TD < PIGD						
Temporal_Sup_L (aal)	BA 22	−63	−30	9	−4.16	53
Parietal_Sup_L (aal)	BA 7	−30	−48	60	−4.44	34
Temporal_Mid_R (aal)	BA 20	42	0	−27	−3.96	50
Temporal_Inf_R (aal)						

TD, tremor-dominant subtype of Parkinson's disease; PIGD, postural instability/gait difficulty subtype of Parkinson's disease; HC, healthy control. BA, Brodmann area; R, right; L, left; Sup, superior; Inf, inferior. All the coordinates are denoted by MNI space coordinates ($P < 0.05$, corrected); AAL, anatomical automatic labeling.

Compared with the controls, the patients with PIGD displayed lower ALFF values in the bilateral putamen, the Crus II of the left cerebellum, the lobule VIII of the right cerebellum, and the cerebellar vermis VIII, and higher ALFF values predominantly in the lobule III, IV, and V of the left cerebellum and some cortical areas, including the right inferior and superior temporal gyrus, the left superior frontal, and parietal gyrus ($P < 0.05$, corrected; Figure 2B and Table 2).

Compared with the patients with PIGD, the patients with TD had higher ALFF values in the lobule VIII of the right cerebellum and the bilateral putamen, but had lower ALFF values in the bilateral temporal gyrus and the left superior parietal lobule ($P < 0.05$, corrected; Figure 2C and Table 2).

Correlation of ALFF Values with Clinical Scores in Patients with PD

For all patients with PD, we further examined correlations of ALFF values with the tremor subscale score and the PIGD subscale score. We found that the tremor score was positively correlated with regional neural activity in the bilateral cerebellar lobule VIII (Figure 3, Table 3). The bilateral putamen and the right cerebellar Crus II showed negative correlations of ALFF values with the PIGD subscale score (Figure 4 and Table 3). We also found that the left putamen showed negative correlation of ALFF values with H-Y stage. No regions showed significant correlation of ALFF values with disease duration in our observation.

Validation Analysis

The Effect of Levodopa

We performed a validation analysis by adding levodopa daily dosage as an additional covariate. ANCOVA revealed significant differences in ALFF among the three groups in the areas of the cerebellar vermis VIII, the right cerebellar lobule VIII, the bilateral putamen, and the right superior frontal gyrus. Comparison between the TD and HC groups also showed similar patterns of ALFF differences as the previous analysis, but with reduced cluster sizes. Meanwhile, comparison between the PIGD and HC groups also revealed significant ALFF differences in the bilateral putamen, the bilateral cerebellar posterior lobe, and the cerebellar vermis VIII. Likewise, comparison between TD and PIGD groups consistently showed significant ALFF differences in the bilateral putamen and the posterior cerebellum (Figure 5). Together, our

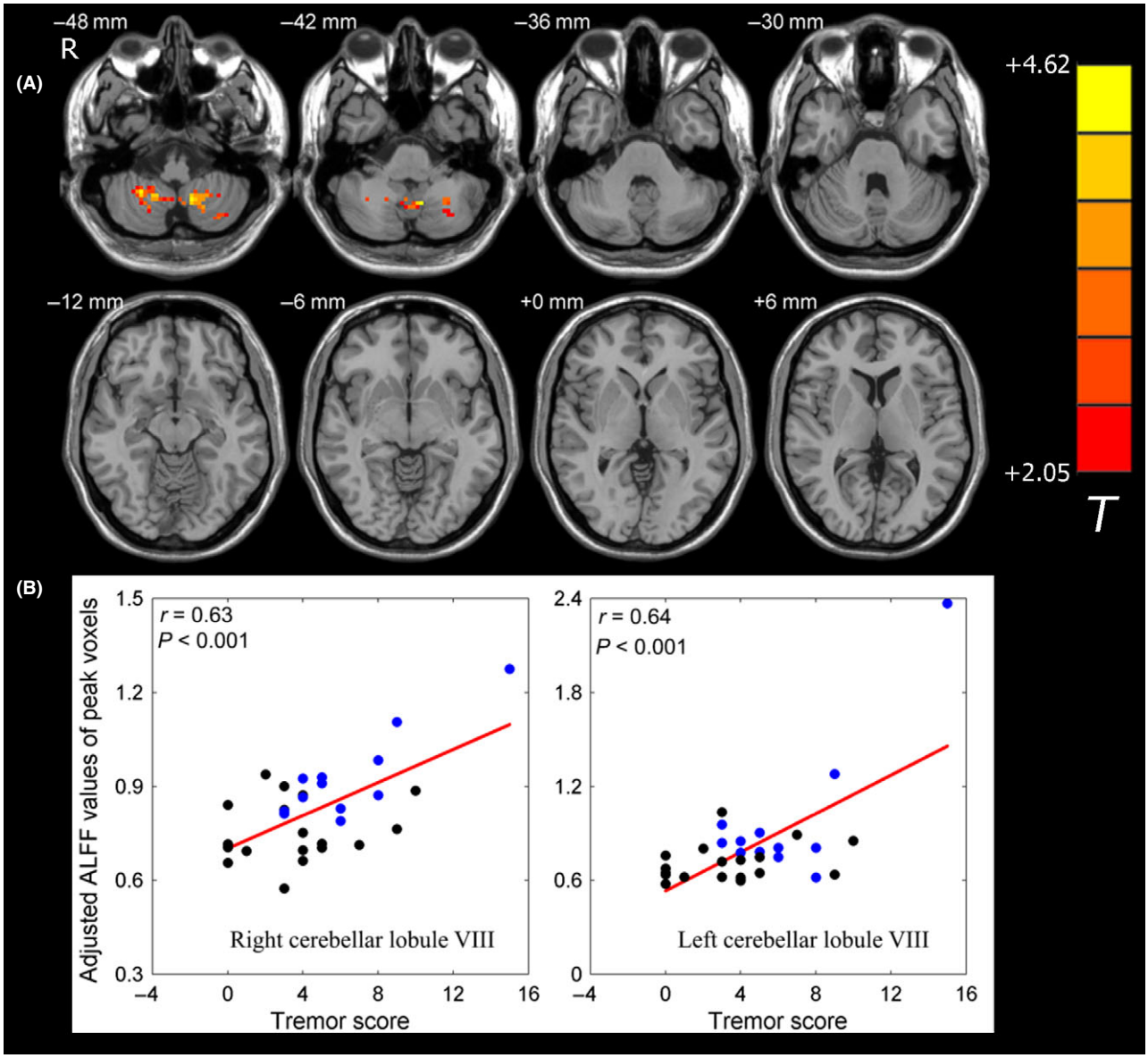

Figure 3 Correlation of ALFF values with tremor score in patients with PD. (**A**) ALFF values in the bilateral cerebellar lobule VIII displayed significant correlation with tremor score in patients with PD. The statistical threshold was set at $P < 0.05$ and cluster size >49 voxels, which corresponds to a corrected $P < 0.05$. (**B**) Scatter plot of ALFF values of peak voxels versus the tremor score of patients with PD. The black dots represent the patients with PIGD, and the blue dots represent the patients with TD.

main results were largely preserved after using levodopa daily dosage as an additional covariate.

The Effect of GM Volume

We first tested differences in GM volumes among the three groups, and no significant difference was found in the current dataset. We further performed a validation analysis by adding GM volume as an additional covariant factor. The brain areas displaying significant ALFF differences among the three groups mainly lied in the bilateral putamen, cerebellar posterior lobe, the left superior frontal gyrus, and the right temporal gyrus. *Post hoc* analysis revealed that the TD group had higher ALFF values in the left superior frontal gyrus, and lower ALFF values in the left insula in comparison with the HC group. Also, compared with the controls, the patients with PIGD showed higher ALFF in the left superior frontal gyrus and the right superior temporal gyrus, and lower ALFF in the bilateral cerebellar Crus I/II, cerebellar lobule VIII, and the bilateral putamen. Comparison between the two subtypes showed that the patients with TD had higher ALFF in the bilateral cerebellar lobule VIII and the bilateral putamen, as well as lower ALFF in the left inferior frontal gyrus (Figure 6). Above all, our main results were largely preserved after using GM volume as an additional covariant factor.

Discussion

In the current study, we employed R-fMRI and ALFF methods to investigate regional differences in spontaneous neural activity in two motor subtypes of PD: TD and PIGD. Our results revealed that compared with controls, patients with TD exhibited higher ALFF values in the right cerebellar lobule VIII and the right superior frontal gyrus, while patients with PIGD exhibited lower ALFF values in the bilateral putamen, the left cerebellar Crus II, the right cerebellar lobule VIII, and the cerebellar vermis VIII, as well as higher ALFF values in the anterior lobe of the left cerebellum and some cortical regions. Relative to patients with PIGD, patients with TD had higher ALFF values in the right cerebellar lobule VIII and the bilateral putamen, as well as lower ALFF values in the bilateral temporal gyrus and the left superior parietal lobule. Moreover, the regional activity in the bilateral cerebellar lobule VIII was positively correlated with tremor severity, and that in the bilateral putamen and the right cerebellar Crus II was negatively correlated with the severity of gait/postural disturbance in patients with PD. These findings provide important insights into the pathophysiological mechanism underlying the two PD subtypes.

Table 3 Correlation of ALFF values with the clinical variables in PD patients

Brain regions	MNI coordinates (mm) x	y	z	*T* value	Cluster size
Correlation of ALFF values with tremor scores					
Cerebellum_8_L (aal)	−12	−57	−51	4.59	46
Cerebellum_8_R (aal)	27	−51	−48	4.53	51
Correlation of ALFF values with PIGD score					
Cerebellum_Crus2_R (aal)	39	−69	−48	−3.75	40
Putamen_R (aal)	33	−6	−27	−3.85	39
Putamen_L (aal)	−24	6	9	−4.76	49
Correlation of ALFF values with H-Y stage					
Putamen_L (aal)	−24	6	9	−4.80	43

We showed that parkinsonian tremor may be associated with higher ALFF values in the cerebellum. In our observations, we found that the patients with TD had higher ALFF values in the right cerebellar lobule VIII compared with both the HC and PIGD groups. Additionally, ALFF values in the bilateral cerebellar lobule VIII were positively correlated with tremor severity in the patients with PD. Previous studies have suggested that PD tremor may be

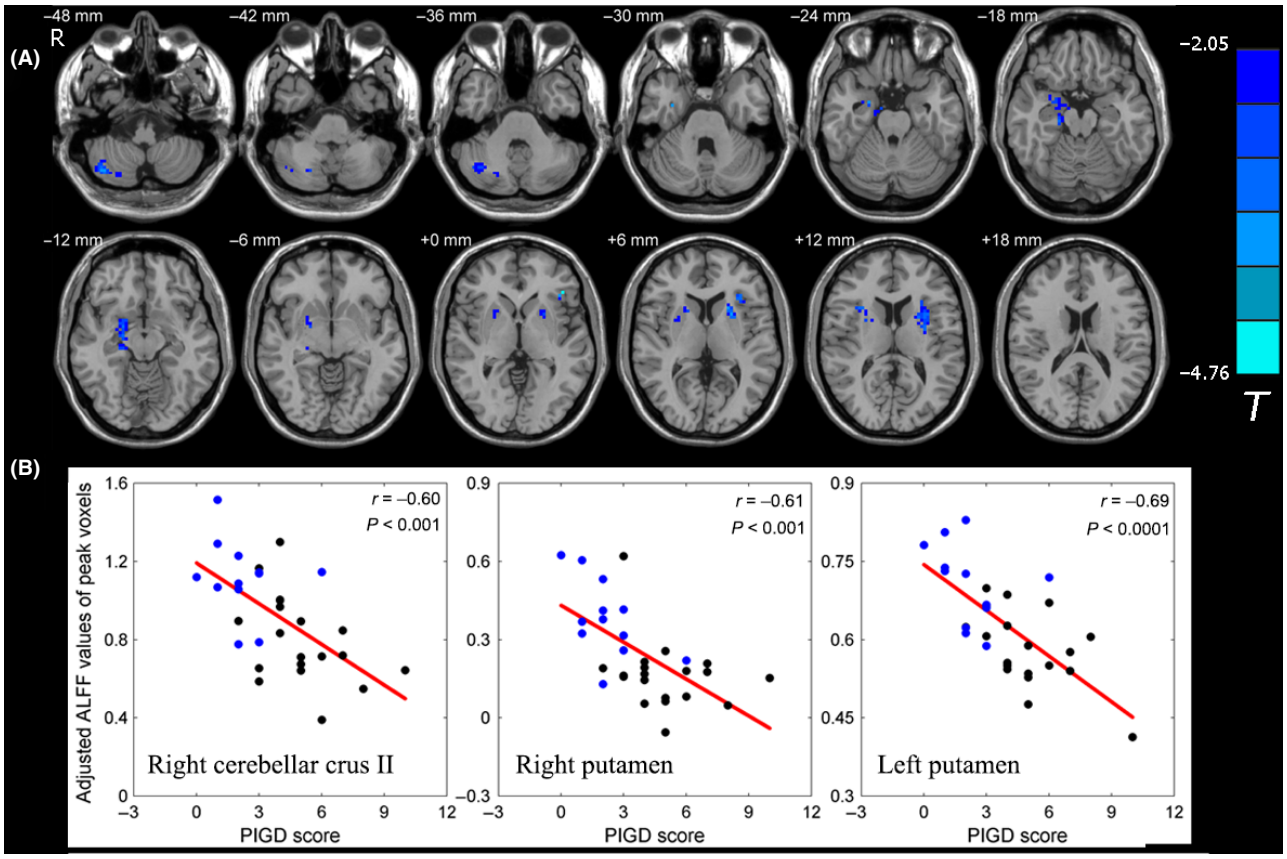

Figure 4 Correlation of ALFF values with PIGD score in patients with PD. (**A**) Correlation maps of PIGD score with ALFF values in patients with PD. The statistical threshold was set at $P < 0.05$ and cluster size >49 voxels, which corresponds to a corrected $P < 0.05$. (**B**) Scatter plot of ALFF values of peak voxels versus the PIGD score of patients with PD. The black dots represent the patients with PIGD, and the blue dots represent the patients with TD.

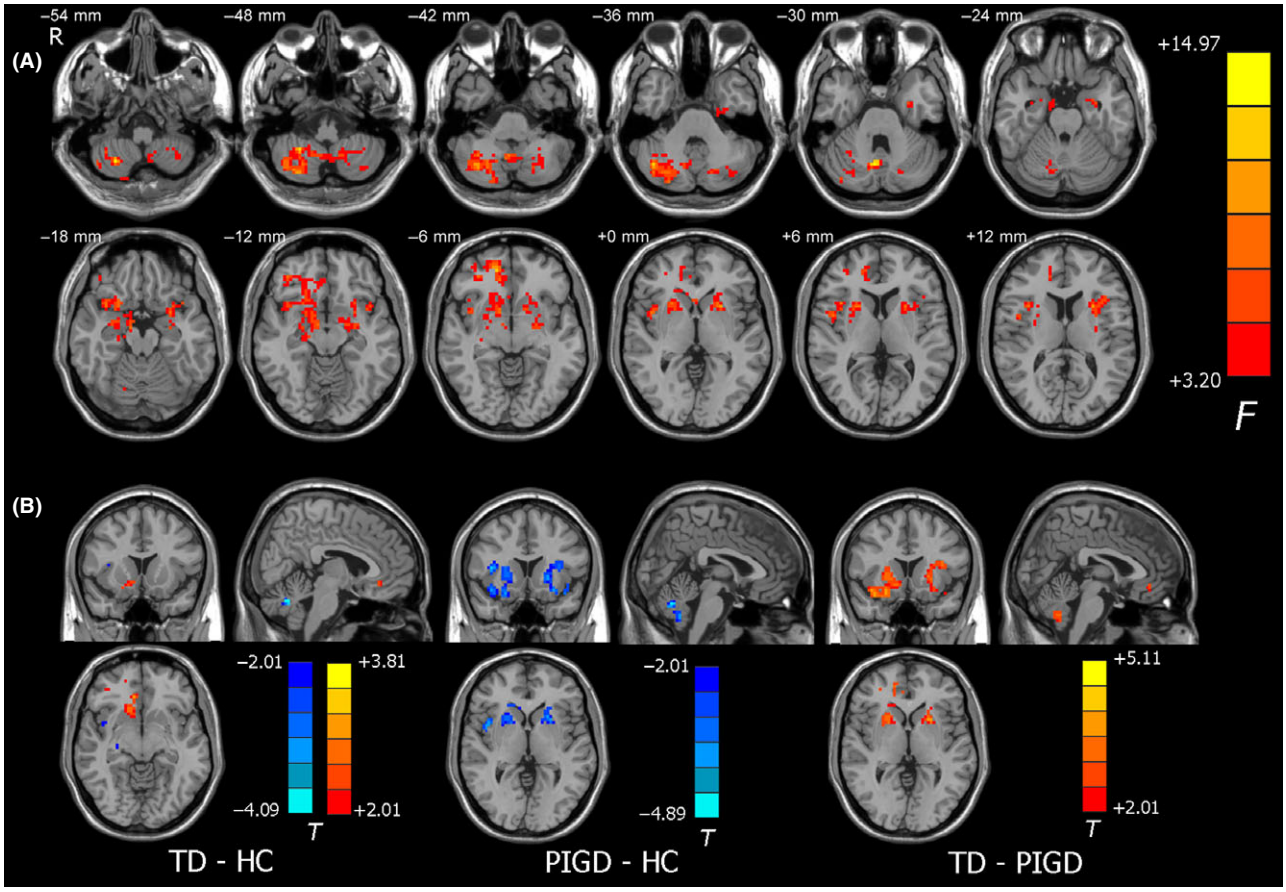

Figure 5 Validation analysis of ALFF differences for levodopa daily dosage. (**A**) Among-group differences with levodopa daily dosage as an additional covariate. The statistical threshold was set at $P < 0.05$ and cluster size >234 voxels, which corresponds to a corrected $P < 0.05$. (**B**) Between-group differences. For comparisons between PIGD and HC groups, and between the PIGD and TD groups, the statistical threshold was set at $P < 0.05$ and cluster size >80 voxels, which corresponds to a corrected $P < 0.05$. Notably, the ALFF difference between the TD and HC groups survived the height threshold, but not the extent threshold; the result displayed here was uncorrected.

driven by the dysfunctional cerebello-thalamo-cortical loop [30], where the cerebellum is an important component. For example, a PET study has identified a PD tremor-related pattern characterized by higher metabolic features in the cerebellar anterior lobe and the M1 area [5], which may support the cerebello-thalamo-cortical hypothesis from a physiological perspective. Several task-based fMRI studies have further postulated that hyperactivity in the cerebellum might be a compensatory effect to overcome defective basal ganglia, which consequently resulted in parkinsonian tremor [31–34]. Such compensatory effects may diminish as pathological damage becomes more severe [35]. Additionally, Helmich and colleagues have used R-fMRI coupling with electromyography and proposed that the cerebellum is one of the circuit sites that are likely to participate in the generation of PD tremor via modulating its amplitude [30]. Our results are compatible with these findings, supporting that hyperactivity in the cerebellum is an underlying feature in the pathophysiology of parkinsonian tremor.

Regarding parkinsonian gait and postural disturbance, we also found that the patients with PIGD had abnormal ALFF values in the cerebellum, where the main affected areas included the right cerebellar lobule VIII, the left cerebellar Crus II, and the cerebellar vermis II. Considering that the cerebellum plays a critical role in regulating ongoing movements and maintaining stable standing posture, it is reasonable to postulate that hypoactivity in the cerebellum may be involved in the gait/postural disturbance in PD. In support of this hypothesis, previous radiotracer studies have consistently reported that greater severity of gait and balance difficulties correlated with more severe cholinergic losses in the brain stem and cerebellum [19,36,37]. Furthermore, pedunculopontine nucleus deep brain stimulation has been proven to be an effective treatment in improving gait and postural symptoms in patients with PD, and a $[^{(15)}O]H_2O$ PET activation study showed that pedunculopontine nucleus deep brain stimulation is associated with increased blood perfusion in the cerebellum [38]. Additionally, a recent fMRI study reported lower GM volumes in the cerebellar declive and culmen of PIGD than TD groups [17]. Accordingly, our study provided direct evidence of regional brain activity alterations for the potential role of cerebellum in the pathophysiology of gait/postural disturbance in PD.

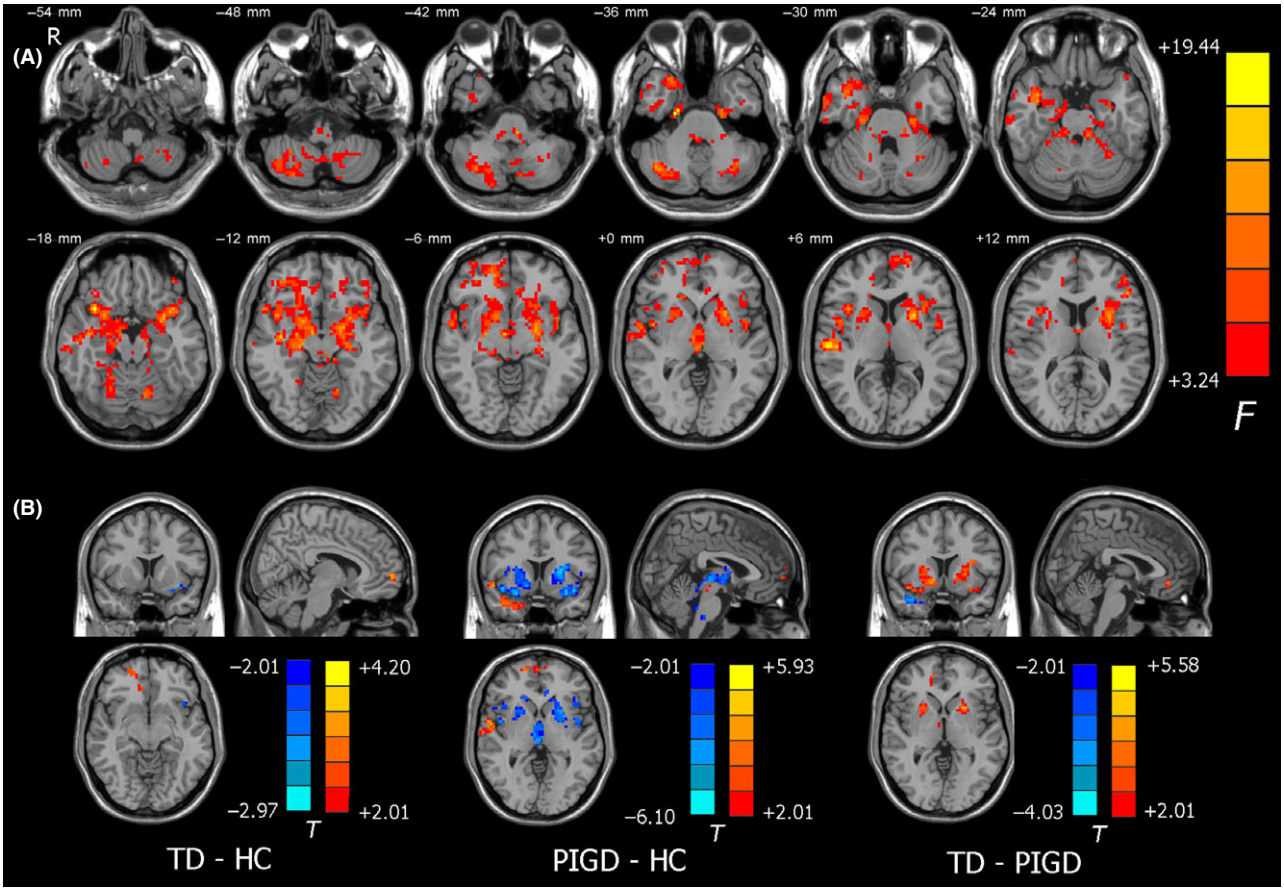

Figure 6 Validation analysis of ALFF differences for GM volume. (**A**) Among-group differences with GM volume as an additional covariate. The statistical threshold was set at $P < 0.05$ and cluster size >283 voxels, which corresponds to a corrected $P < 0.05$. (**B**) Between-group differences of *post hoc* analysis. For comparisons between PIGD and HC groups, and between the PIGD and TD groups, the statistical threshold was set at $P < 0.05$ and cluster size >59 voxels, which corresponds to a corrected $P < 0.05$. The result of comparison between the TD and HC groups was uncorrected.

Moreover, we also found that the patients with PIGD had lower ALFF values in the bilateral putamen than both controls and patients with TD. Generally, the putamen is thought to control several types of motor skills, such as motor learning, motor preparation, and movement sequences. It has been indicated that the dysfunctional putamen in PD might result in difficulty of performance of previously learned movements [39]. Previously, in a neuroimaging study, it was reported that depletion of dopamine projection in the striatum affects the putamen most severely [40]. More recently, fMRI studies have also found that the putamen is significantly affected in patients with PD [41,42], and have consistently reported lower regional neural activity in the putamen [43,44]. Our results are not only compatible with these observations, but also provide evidence that regional neural activity in the putamen can distinguish between motor subtypes of PD, where patients with PIGD seem to be more affected. Compared with the TD subtype, the PIGD subtype has been shown to have more impaired presynaptic dopamine function in the putamen in a SPECT study, which further supports our observation [6]. Such heterogeneity in the putamen may suggest that an impaired putamen may be associated with gait/postural disturbance. Further correlation analysis could support this hypothesis by showing that ALFF values in the bilateral putamen are negatively correlated with PIGD subscale scores in all patients with PD. Taken together, we speculate that an impaired putamen may underlie the pathophysiology of gait/postural disturbance in PD.

Our results also showed lower regional neural activity in the brain stem in patients with PIGD compared with controls. Although such a change was not detected in patients with TD, it could not be excluded because the sample size of this group was relatively smaller. Thus, lower ALFF in the brain stem is at least a feature of PD. According to the classic Braak stage, pathological alterations occur primarily in the brain stem, pursue an ascending course, and reach the neocortex in the final stage [45]. Therefore, our results conform to the classic pathological changes in the brain stem in patients with PD. Other fMRI studies have also been suggestive of brain stem dysfunction in patients with PD. For example, Hacker et al. (2012) performed functional connectivity analysis of the striatum in PD and found that the functional connectivity between the brain stem and the striatum was remarkably lower in patients with PD compared with healthy controls [46]. Besides, Hou et al. (2014) investigated the regional activity pattern of PD in the slow-4 and slow-5 frequency bands and found that patients with PD had higher ALFF values in the midbrain in

both frequency bands [11]. We also found lower ALFF values in the brain stem, while it located in the lower part of the pons and the top of the medulla instead of the midbrain. This discrepancy implies that multiple levels of the brain stem may have different patterns of spontaneous neural activity in PD. However, such a hypothesis needs to be further tested.

Furthermore, multiple cortical regions showed distinct changes in ALFF values in patients with PD in our study, including the bilateral prefrontal cortex and the left superior parietal lobule. To begin with, the bilateral prefrontal cortex is involved in strategic processing in attention and high-order cognitive functions [47]. R-fMRI studies have revealed impaired functional connectivity between the prefrontal cortex and the putamen [41] and have also shown the regional hyperactivity in the prefrontal cortex in patients with PD [15,48]. Our results are in keeping with these observations. It is noteworthy that after adding levodopa daily dosage as a covariate in our analysis, the prefrontal cortex did not show a significant ALFF difference among groups. It could be said that the alteration of regional neural activity in the prefrontal cortex might result from long-term drug effects, instead of primary pathophysiological changes. Another significant finding was that patients with PIGD had higher ALFF values in the left superior parietal lobule than the HC and TD groups. The superior parietal lobule is believed to engage in visual processing, and evidence has shown that PD patients with hallucination have lower ALFF values in the primary visual cortex, as well as higher ALFF values in the temporo-parietal area including the superior parietal lobule [49]. Actually, patients with PIGD have higher tendency to develop visual hallucination than patients with TD in clinical observation [50], and we speculate that it may be associated with the alteration of regional neural activity in the superior parietal cortex. Of note, the ALFF difference in the superior parietal cortex was also eliminated after adding levodopa daily dosage as an additional covariate, which could be interpreted that higher ALFF values in the superior parietal lobule may also be due to long-term drug effects. And in clinical practice, levodopa daily dosage itself is believed to be a risk factor for PD hallucination [51]. Therefore, we speculate that there might be associations among PD hallucination, long-term levodopa administration, and the hyperactivity in the superior parietal lobule, which need to be further investigated. In addition, the potential difference in GM volume was also tested among groups and no significant difference was found. This result is consistent with clinical findings, where the cognitive dysfunction is only observed in advanced PD and the brain atrophy is rarely observed in early period of disease duration. In our patients, the mean disease duration is around 6 years, mean HY around 2, and MMSE above 24. After taking GM volume as an additional covariate, our main results can be preserved.

Finally, there are some limitations in our study. First, the sample size for each subtype is relatively small, especially for the TD subtype. As a result, the primary threshold within a single cluster was set at $P < 0.05$, which might be loose. A large sample size may be needed if a strict threshold is applied in the future. Second, the normalization of cerebellum is an important concern in deciphering the functions of different cerebellar regions; thus, a better strategy remains to be established to investigate the involvement of the cerebellum in PD. Third, a significant correlation does not confirm causation; a longitudinal observation in combination with the effects of drug and deep brain stimulation treatments is needed to offer more evidence.

Conclusion

Our findings suggest different patterns of regional spontaneous brain activity in the cerebellum and putamen in the two PD subtypes: TD and PIGD. We conclude that hyperactivity in the cerebellum may underlie the neural substrate of parkinsonian tremor and that hypoactivity in the cerebellum and the putamen may underlie the pathophysiology of gait/postural disturbance of PD. Further investigations into the longitudinal changes in spontaneous brain activity during disease progression and after treatment interventions are needed in the future.

Acknowledgment

This research was supported by Beijing Nature Science Foundation and Beijing Municipal Commission of Education, China (Grant No. kz20120025028), National Key Technology Research and Development Program of the Ministry of Science and Technology of China (Grant No. 2013BAI09B03), and Beijing Institute for Brain Disorders (BIBD-PXM2013_014226_07_000084).

Conflict of Interest

The article has not been published or submitted elsewhere. The authors declare no conflict of interest.

Reference

1. Jankovic J, McDermott M, Carter J, et al. Variable expression of Parkinson's disease: A base-line analysis of the DATATOP cohort. The Parkinson Study Group. *Neurology* 1990;**40**:1529–1534.
2. Rajput AH, Pahwa R, Pahwa P, Rajput A. Prognostic significance of the onset mode in parkinsonism. *Neurology* 1993;**43**:829–830.
3. Mehanna R, Lai EC. Deep brain stimulation in Parkinson's disease. *Transl Neurodegener* 2013;**2**:22.
4. Jankovic J, Kapadia AS. Functional decline in Parkinson disease. *Arch Neurol* 2001;**58**:1611–1615.
5. Mure H, Hirano S, Tang CC, et al. Parkinson's disease tremor-related metabolic network: Characterization, progression, and treatment effects. *NeuroImage* 2011;**54**:1244–1253.
6. Mo SJ, Linder J, Forsgren L, Larsson A, Johansson L, Riklund K. Pre- and postsynaptic dopamine SPECT in the early phase of idiopathic parkinsonism: A population-based study. *Eur J Nucl Med Mol Imaging* 2010;**37**:2154–2164.
7. Biswal B, Yetkin FZ, Haughton VM, Hyde JS. Functional connectivity in the motor cortex of resting human brain using echo-planar MRI. *Magn Reson Med* 1995;**34**:537–541.
8. Fox MD, Raichle ME. Spontaneous fluctuations in brain activity observed with functional magnetic resonance imaging. *Nat Rev Neurosci* 2007;**8**:700–711.
9. Zhang D, Raichle ME. Disease and the brain's dark energy. *Nat Rev Neurol* 2010;**6**:15–28.
10. Zang YF, He Y, Zhu CZ, et al. Altered baseline brain activity in children with ADHD revealed by resting-state functional MRI. *Brain Dev* 2007;**29**:83–91.
11. Hou Y, Wu X, Hallett M, Chan P, Wu T. Frequency-dependent neural activity in Parkinson's disease. *Hum Brain Mapp* 2014;**35**:5815–5833.
12. Liu X, Wang S, Zhang X, Wang Z, Tian X, He Y. Abnormal amplitude of low-frequency fluctuations of intrinsic brain activity in Alzheimer's disease. *J Alzheimers Dis* 2014;**40**:387–397.
13. Hoptman MJ, Zuo XN, Butler PD, et al. Amplitude of low-frequency oscillations in schizophrenia: A resting state fMRI study. *Schizophr Res* 2010;**117**:13–20.
14. Skidmore FM, Yang M, Baxter L, et al. Reliability analysis of the resting state can sensitively and specifically identify

the presence of Parkinson disease. *NeuroImage* 2013;**75**:249–261.
15. Zhang J, Wei L, Hu X, et al. Akinetic-rigid and tremor-dominant Parkinson's disease patients show different patterns of intrinsic brain activity. *Parkinsonism Relat Disord* 2015;**21**:23–30.
16. Gu Q, Huang P, Xuan M, et al. Greater loss of white matter integrity in postural instability and gait difficulty subtype of Parkinson's disease. *Can J Neurol Sci* 2014;**41**:763–768.
17. Rosenberg-Katz K, Herman T, Jacob Y, Giladi N, Hendler T, Hausdorff JM. Gray matter atrophy distinguishes between Parkinson disease motor subtypes. *Neurology* 2013;**80**:1476–1484.
18. Muller ML, Frey KA, Petrou M, et al. beta-Amyloid and postural instability and gait difficulty in Parkinson's disease at risk for dementia. *Mov Disord* 2013;**28**:296–301.
19. Bohnen NI, Frey KA, Studenski S, et al. Gait speed in Parkinson disease correlates with cholinergic degeneration. *Neurology* 2013;**81**:1611–1616.
20. Hughes AJ, Daniel SE, Kilford L, Lees AJ. Accuracy of clinical diagnosis of idiopathic Parkinson's disease: A clinico-pathological study of 100 cases. *J Neurol Neurosurg Psychiatry* 1992;**55**:181–184.
21. Chao-Gan Y, Yu-Feng Z. DPARSF: A MATLAB Toolbox for "Pipeline" Data Analysis of Resting-State fMRI. *Front Syst Neurosci* 2010;**4**:13.
22. Collignon A, Maes F, Delaere D, Vandermeulen D, Suetens P, Marchal G. *Automated Multi-Modality Image Registration Based on Information Theory*. Dordrecht, The Netherlands: Kluwer Academic Publishers, 1995.
23. Ashburner J, Friston KJ. Unified segmentation. *NeuroImage* 2005;**26**:839–851.
24. Friston KJ, Frith CD, Frackowiak RS, Turner R. Characterizing dynamic brain responses with fMRI: A multivariate approach. *NeuroImage* 1995;**2**:166–172.
25. Lowe MJ, Mock BJ, Sorenson JA. Functional connectivity in single and multislice echoplanar imaging using resting-state fluctuations. *NeuroImage* 1998;**7**:119–132.
26. Jenkinson M, Bannister P, Brady M, Smith S. Improved optimization for the robust and accurate linear registration and motion correction of brain images. *NeuroImage* 2002;**17**:825–841.
27. Song XW, Dong ZY, Long XY, et al. REST: A toolkit for resting-state functional magnetic resonance imaging data processing. *PLoS ONE* 2011;**6**:e25031.
28. Yang H, Long XY, Yang Y, et al. Amplitude of low frequency fluctuation within visual areas revealed by resting-state functional MRI. *NeuroImage* 2007;**36**:144–152.
29. Ashburner J. A fast diffeomorphic image registration algorithm. *NeuroImage* 2007;**38**:95–113.
30. Helmich RC, Janssen MJ, Oyen WJ, Bloem BR, Toni I. Pallidal dysfunction drives a cerebellothalamic circuit into Parkinson tremor. *Ann Neurol* 2011;**69**:269–281.
31. Wu T, Liu J, Zhang H, Hallett M, Zheng Z, Chan P. Attention to Automatic Movements in Parkinson's Disease: Modified Automatic Mode in the Striatum. *Cereb Cortex* 2014. [Epub ahead of print].
32. Yu H, Sternad D, Corcos DM, Vaillancourt DE. Role of hyperactive cerebellum and motor cortex in Parkinson's disease. *NeuroImage* 2007;**35**:222–233.
33. Wu T, Wang L, Hallett M, Li K, Chan P. Neural correlates of bimanual anti-phase and in-phase movements in Parkinson's disease. *Brain* 2010 Aug;**133**(Pt 8):2394–2409.
34. Lewis MM, Du G, Sen S, et al. Differential involvement of striato- and cerebello-thalamo-cortical pathways in tremor- and akinetic/rigid-predominant Parkinson's disease. *Neuroscience* 2011;**177**:230–239.
35. Wu T, Hallett M. The cerebellum in Parkinson's disease. *Brain* 2013;**136**(Pt 3):696–709.
36. Bohnen NI, Frey KA, Studenski S, et al. Extra-nigral pathological conditions are common in Parkinson's disease with freezing of gait: An in vivo positron emission tomography study. *Mov Disord* 2014;**29**:1118–1124.
37. Gilman S, Koeppe RA, Nan B, et al. Cerebral cortical and subcortical cholinergic deficits in parkinsonian syndromes. *Neurology* 2010;**74**:1416–1423.
38. Ballanger B, Lozano AM, Moro E, et al. Cerebral blood flow changes induced by pedunculopontine nucleus stimulation in patients with advanced Parkinson's disease: A [(15)O] H2O PET study. *Hum Brain Mapp* 2009;**30**:3901–3909.
39. Griffiths PD, Perry RH, Crossman AR. A detailed anatomical analysis of neurotransmitter receptors in the putamen and caudate in Parkinson's disease and Alzheimer's disease. *Neurosci Lett* 1994;**169**:68–72.
40. Brooks DJ, Ibanez V, Sawle GV, et al. Differing patterns of striatal 18F-dopa uptake in Parkinson's disease, multiple system atrophy, and progressive supranuclear palsy. *Ann Neurol* 1990;**28**:547–555.
41. Helmich RC, Derikx LC, Bakker M, Scheeringa R, Bloem BR, Toni I. Spatial remapping of cortico-striatal connectivity in Parkinson's disease. *Cereb Cortex* 2010;**20**:1175–1186.
42. Herz DM, Eickhoff SB, Lokkegaard A, Siebner HR. Functional neuroimaging of motor control in Parkinson's disease: A meta-analysis. *Hum Brain Mapp* 2014;**35**:3227–3237.
43. Wu T, Long X, Zang Y, et al. Regional homogeneity changes in patients with Parkinson's disease. *Hum Brain Mapp* 2009;**30**:1502–1510.
44. Yang H, Zhou XJ, Zhang MM, Zheng XN, Zhao YL, Wang J. Changes in spontaneous brain activity in early Parkinson's disease. *Neurosci Lett* 2013;**549**:24–28.
45. Braak H, Del Tredici K, Rub U, de Vos RA, Jansen Steur EN, Braak E. Staging of brain pathology related to sporadic Parkinson's disease. *Neurobiol Aging* 2003;**24**:197–211.
46. Hacker CD, Perlmutter JS, Criswell SR, Ances BM, Snyder AZ. Resting state functional connectivity of the striatum in Parkinson's disease. *Brain* 2012 Dec;**135**(Pt 12):3699–3711.
47. Ramnani N, Owen AM. Anterior prefrontal cortex: Insights into function from anatomy and neuroimaging. *Nat Rev Neurosci* 2004;**5**:184–194.
48. Hu XF, Zhang JQ, Jiang XM, et al. Amplitude of low-frequency oscillations in Parkinson's disease: A 2-year longitudinal resting-state functional magnetic resonance imaging study. *Chin Med J (Engl)* 2015;**128**:593–601.
49. Yao N, Pang S, Cheung C, et al. Resting activity in visual and corticostriatal pathways in Parkinson's disease with hallucinations. *Parkinsonism Relat Disord* 2015;**21**:131–137.
50. Auyeung M, Tsoi TH, Mok V, et al. Ten year survival and outcomes in a prospective cohort of new onset Chinese Parkinson's disease patients. *J Neurol Neurosurg Psychiatry* 2012;**83**:607–611.
51. Zhu K, van Hilten JJ, Putter H, Marinus J. Risk factors for hallucinations in Parkinson's disease: Results from a large prospective cohort study. *Mov Disord* 2013;**28**:755–762.

